

<https://doi.org/10.33472/AFJBS.6.5.2024.5773-5791>



African Journal of Biological Sciences



Formulation Development, Optimisation In Vitro & In Vivo Evaluation Of Antiretroviral Drug Loaded Goldnanoparticles By Using Box–Behnken Design

Mrs. Nagalakshmi Ponnada^{1*}, Dr. P. Shailaja¹, Dr. G. Girija Sankar²

¹Research Scholar, A U College of Pharmaceutical Sciences, Andhra University, Visakhapatnam – 530003.

Email: laxmiponnada@gmail.com¹

¹Associate Professor, A U College of Pharmaceutical Sciences, Andhra University, Visakhapatnam – 530003.

²Professor, A U College of Pharmaceutical Sciences, Andhra University, Visakhapatnam – 530003.

***Corresponding Author:** Mrs. Nagalakshmi Ponnada

*Email: laxmiponnada@gmail.com

Article History

Volume 6, Issue 5, May 2024

Received: 05 may 2024

Accepted: 12 may 2024

Doi: 10.33472/AFJBS.6.5.2024.5773–5791

ABSTRACT

The effective and preventive treatment of HIV is one of the difficult challenges worldwide. It requires the development of an effective prophylactic strategy to prevent HIV/AIDS. ATV has been successfully used in treatment-naïve and experienced HIV patients. ATV belongs to Biopharmaceutics Classification System (BCS) class II drug with poor water solubility and high permeability (log P of 4.11). ATV undergoes rapid first-pass metabolism and P-gp efflux, leading eventually to marked reduction in the drug oral bioavailable fraction (i.e. 60%) in humans and animals. To circumvent the a fore mentioned limitations various formulation approaches of ATV have been reported like, Nanocrystals, tablets and capsules but all with limited fruition. It has been well reported in the literature that daily dose of ATV causes serious liver problems, specifically hepatotoxicity. As a shortfall for all the conventional oral dosage forms, the duration of action is limited since the absorption of the drug depends on the resident time of the drug in the gastrointestinal tract. In order to fulfill the need of a long-term treatment with anti HIV agents, where most of them suffer from the shortcoming of frequent administration and plasma concentration fluctuation, it is desirable to have novel drug-delivery carriers such as NPs. This study aimed to develop Atazanavir –biodegradable gold (Au) nanoparticles by using pectin as a reducer and stabilizer. ATZ–GNPs were prepared by the slightly modified Turkevich et al method. ATZ–GNPs were optimized using Box Behnken design for independent variables gold chloride (A), pectin (B) and pH range (C). The effects of independent variables were observed on particle size (Y¹) and encapsulation efficiency (Y²).The results of the study revealed that the optimized nanoparticles (GLN7) had a particle size of 3.9 ± 0.1 nm and encapsulation efficiency of $97.2 \pm 3.9\%$. TEM study showed the spherical shape particles. The in-vitro drug release revealed $99.84 \pm 0.23\%$ in phys- iological buffer (pH 7.4). In-vitro cytotoxicity study and antibacterial activity depicted the safety of the prepared NPs by showing lesser toxicity than pure ATZ. From the results, our experimental outcomes concluded that ATZ gold nanoparticles composed of pectin may constitute a preferred embodiment for the

delivery of ATZ.

Keywords: Atazanavir, Goldnanoparticles, Box-Behnken, pectin.

INTRODUCTION:

Gold nanoparticles provide an excellent material for study the most stable, non-toxic and easy to synthesize nanoparticles and it exhibits various interesting properties such as aggregation type and quantum size effect. The optical behavior of gold nanoparticles depends on surface plasmon resonance (SPR). wide area from visible to infrared area The spectrum is determined by mass oscillations transfer electrons. The range of the spectrum depends different properties of gold nanoparticles, size and Fig.9 A method has been developed to synthesize this material that can be changed by increased use chemical functional groups are innumerable. Many new sensations and special studies based on gold nanoconjugates. Gold nanoparticles have emerged as practical candidates for the delivery of various cargo carriers to the target place. This is a small carrier drug molecules including drugs for large biomolecules such as DNA, RNA and protein. Some drug molecules do not requires modification of the gold nanoparticle monolayer can be directly connected to gold for delivery physical absorption with ions or nanoparticles covalent bonds. To be sent by others charge carriers require functionality such as gold nanoparticles PEGylation, peptide and amino acid conjugation or work with oligonucleotides. In addition, another prerequisite for effective delivery of therapeutic agents is their release. Various internal stimuli (glutathione, pH, and enzymes) and external stimuli (light, etc.) as investigated for effective release gold nanoparticles. Because of the abundance of information available and we choose the renewable level data is summarized over the past few years to illustrate this include the most promising programs Gold nanoparticles in drug delivery.¹⁻³

Pre-formulation studies:

Prior to the development of dosage form, it is essential that certain fundamental physical and chemical properties of the drug molecule alone and when combined with excipients are determined. This first learning phase is known as pre-formulation. The overall objective of the pre-formulation is to generate information useful to the formulator in developing stable and bioavailable dosage forms which can be mass produced.^{1,2}

The goals of pre-formulation studies are:

- To evaluate the drug substance analytically and determine its necessary characteristics
- To establish its compatibility with different excipients.^{1,2}

1.2 Spectroscopic study:

1.2.1 Melting Point:

The temperature at which the first particle of the substance completely melts is regarded as melting point of the substance. The temperature at which the first particle starts to melt and last particle completely melts is regarded as the range of melting point. The melting point of Atazanavir was found to be in range of 168°C 170°C. which was determined by capillary method by usin SSU Melting point apparatus,

1.2.2 Solubility studies: –

Solubility of Atazanavir was carried out in different solvents –like water, 0.1 N HCl, pH 6.8 Phosphate buffer, pH 7.4 phosphate buffer .Saturated solutions were prepared by adding excess drug to the vehicles and shaking on the shaker for 48 hr. at 25°C under constant vibration.

Filtered samples (1 ml) were diluted appropriately with pH 7.4 buffer and solubility of Atazanavir was determined spectrophotometrically at 292 nm.^{3,5,6,7}

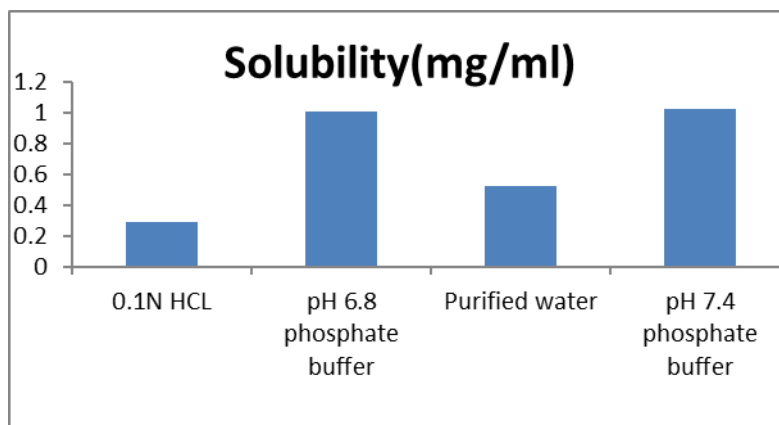


Fig: 1.1 Solubility Studies of Atazanavir

1.2.3 Drug–Excipient Interactions Studies: There is always possibility of drug– excipient interaction in any formulation due to their intimate contact. The technique employed in this study is IR spectroscopy. IR spectroscopy is one of the most powerful analytical technique, which offers possibility of chemical identification. The IR spectra was obtained by KBr pellet method. (Perkin–Elmer series 1615 FTIR Spectrometer).⁴

1.2.4 Determination of absorption maximum (λ_{max}):

The wavelength at which maximum absorption of radiation takes place is called as λ_{max} . For accurate analytical work, it is important to determine the absorption maxima of the substance under study. Most drugs absorb radiation in ultraviolet region (190–390 nm), as they are aromatic or contain double bonds.

Accurately weighed 10 mg of Atazanavir was dissolved in pH 7.4 buffer taken in a clean 10 ml volumetric flask. The volume was made up to 10 ml with the same which will give stock solution–I with concentration 1000 $\mu\text{g/ml}$. From the stock solution–I, 1 ml was pipette out in 10ml volumetric flask. The volume was made up to 10 ml using pH 6.8 buffer to obtain stock solution–II with a concentration 100 $\mu\text{g/ml}$. From stock solution–II, 1ml was pipette out in 10ml volumetric flask. The volume was made up to 10ml using pH 7.4 buffer to get a concentration of 10 $\mu\text{g/ml}$. This solution was then scanned at 200–400nm in UV–Visible double beam spectrophotometer to attain the absorption maximum (λ_{max}).

1.2.5 Preparation of calibration curve of atazanavir

Procedure for standard curve in pH 7.4:

10 mg of Atazanavir was dissolved in 10 ml of pH 7.4 by slight shaking (1000 mcg/ml). 1 ml of this solution was taken and made up to 10 ml with pH 7.4, which gives 100 mcg/ ml concentration (stock solution). From the stock solution, concentrations of 2, 4, 6, 8, 10 and 12 $\mu\text{g/ml}$ in pH 7.4 were prepared. The absorbance of diluted solutions was measured at 292 nm and a standard plot was drawn using the data obtained.

1.3 Design of Experiment:

In the present study, Box–Behnken design (Design Expert® 12, Statease) has been employed to optimize the gold NPs (GNPs).The optimization was performed using 3 factors: gold chloride

(A), pectin (B), and solution pH (C) at 3 levels (low, medium, high). The effect of independent variables was evaluated on the dependent variables as PS (Y^1) and EE (Y^2). The design showed 15 formulation runs with 3 common compositions to check the error during the preparation. The different models like linear, quadratic and 2F were used to evaluate the optimization process. The ideal model for the selection of optimized formulation is the quadratic model in which the selected independent variables showed the individual as well as combined effects. The p-value of the regression coefficient was also used to evaluate the significant factors over the responses. Further, ANOVA was also applied to determine the significance of the model. The software generated polynomial equation of each factor was used to evaluate the negative and positive effects on the PS and EE⁶. The predicted and actual value of each response was used to validate the method. Finally, the selected optimized NPs were characterized for physicochemical properties.

Table 1.2: BoxBehnken design based experimental runs and their responses used for the formulation of ATZ gold nanoparticles

Formulation Code	Independent variables			Responses (Mean \pm SD;n=3)		
	ATZ mg	Gold chloride (mM);X ¹	Pectin(%);X ²	pH;X ³	Particle Size (nm);Y ¹	Entrapment efficiency (%);Y ²
GLN-1	400	1	1.00	12	17.1 \pm 0.1	82.7 \pm 1.4
GLN-2	400	3	0.51	11	65.3 \pm 0.3	57.4 \pm 2.9
GLN-3	400	2	0.51	12	34.5 \pm 0.2	72.5 \pm 1.3
GLN-4	400	3	1.00	12	86.8 \pm 0.3	65.9 \pm 2.5
GLN-5	400	2	0.01	13	31.7 \pm 0.2	79.5 \pm 3.1
GLN-6	400	3	0.51	13	78.1 \pm 0.2	68.7 \pm 2.4
GLN-7	400	1	0.01	12	3.1 \pm 0.2	94.1 \pm 1.3
GLN-8	400	1	0.51	11	7.5 \pm 0.2	89.8 \pm 1.7
GLN-9	400	2	0.51	12	34.1 \pm 0.3	71.9 \pm 2.1
GLN-10	400	2	0.51	12	35.9 \pm 0.2	71.1 \pm 1.9
GLN-11	400	2	0.01	11	25.8 \pm 0.1	77.8 \pm 1.7
GLN-12	400	2	0.51	13	9.4 \pm 0.2	86.2 \pm 2.9
GLN-13	400	2	1.00	13	51.9 \pm 0.1	73.7 \pm 3.2
GLN-14	400	2	1.00	11	44.8 \pm 0.3	67.4 \pm 3.2
GLN-15	400	3	0.01	12	65.2 \pm 0.2	63.1 \pm 1.7

1.4 Method of Preparation:

1.4.1 Fabrication of Gold Nanoparticles

The slightly modified reported method by nanoprecipitation was used to synthesize ATZ gold NPs. The colloidal dispersion of AuCl₄ was prepared by the reduction of tetrachloroauric acid (gold chloride). Different concentration of gold chloride (1 to 3 mM) was added to pectin solution in a concentration of 0.01 to 1% (w/v) for 10–15 min at a basic pH range of 11–13. The prepared dispersion was converted to ruby red from blue colour. The synthesised gold NPs were dialyzed for 12 h with double distilled water in which the dispersion of the pH was found to be 7. A calculated amount of drug (ATZ) was dispersed in tween 60 solution (0.1 nmol/L) and then added to a gold NPs dispersion with a resultant ATZ concentration of 5 mM in 100 mL solution. The concentration of each variable used to prepare gold NPs are mentioned in Table 4.1. The mixture was incubated for 24 h at room temperature and then centrifuged at 30,000 rpm for 2 h to remove excess drug. The collected pellet was separated from the supernatant solution and redispersed in water for further characterization.⁸

1.5 Optimization:

ATZ–GNPs were prepared and further optimized using Box Behnken design. The variables used to optimize gold chloride (A), pectin (B) and pH (C) are shown in Table 1. These variables were taken at three–level (low, medium, high) and the formulation composition effects were assessed on PS (Y¹) and EE (Y²) (Fig. 1A,B). For every formulations; size, PDI, zeta potential and encapsulation efficiency were evaluated. The factors which got significantly affected by the variation of the independent variables were selected for the optimization process. It was found that the result of PDI and ZP have no significant effect. The design showed 15 different compositions with three common formulae to check the error. The optimization was performed using different mathematical models (linear, 2 F1, quadratic and cubic) given by the software. The quadratic model is considered an ideal model because it shows the individual as well as a combined effect of the used variable on the PS and EE. The results revealed the highest values for both adjusted and predicted regression coefficients and considered as a best–fit model (0.9), of independent variables. The effect of independent variables on the PS could be well observed from the polynomial equation and 3D response surface plot (Fig.5.4) in results and discussion.

1.6 Evaluation parameters of Atazanavir Gold Nanoparticles:^{9–16}

The Atazanavir Gold Nanoparticles was evaluated for various parameters:–

1. Particle size(PS) , Polydispersity Index (PDI) and Surface Charge (ZP) .
2. Entrapment efficiency.
3. Percentage yield.
4. Drug content.
5. Transmission electron microscopy (TEM). Scanning electron microscopy(SEM).
6. XRD Analysis.
7. In–vitro drug release studies.
8. Antibacterial activity.
9. Cytotoxic study.

1.6.1 Particle size (PS), Poly dispersity Index (PDI) and Surface charge (ZP):

The prepared ATZ–GNPs were evaluated for PS, PDI and ZP using a particle size analyzer (Malvern Zetasizer, Malvern, UK). PDI is used to measure the particle size distribution and the value below 0.7 is considered uniform.^{1–3} GLN–7 (0.1 ml) was dispersed in double distilled water and transferred to a cuvette for the analysis. The same sample was taken in the cuvette with an electrode to measure the ZP.

1.6.2 Encapsulation efficiency (% EE):

The experiment was carried out to evaluate the amount of ATZ encapsulated in the prepared nanoparticles by the indirect method. The sample of GLN–7 (2 ml) was taken and centrifuged for one hour at 10,000 rpm. The supernatant of the centrifuged dispersion was taken, diluted, and assayed spectrophotometrically (Perkin Elmer, LAMDA– 35) at 537 nm. Each formulation was evaluated three times and the mean encapsulation efficiency was evaluated using the formula:

$$\% \text{Encapsulation efficiency} = \frac{\text{Weight of initial ATZ} - \text{Weight of free ATZ}}{\text{Weight of initial ATZ}}$$

1.6.3 Percentage Yield:

The prepared ATZ–GNPs (GLN–7) were collected and weighed accurately to evaluate the percentage yield. The individual weight of each ingredient was also taken to

calculatethepercentageyieldofthenanoparticlesusingthe following Eq. ⁶

% Yield = $T_m / T_i \times 100$ T_m total weight of dried nanoparticles; T_i total dry weight of all added components.

Drug content:

1 gm of Atazanavir GNPs were accurately weighed and transferred into a 25ml volumetric standard flask. The sample was dissolved with pH 7.4 phosphate buffer solution. 1ml of this solution was diluted to 25 ml with the same buffer solution. The standard Atazanavir was dissolved and diluted with same buffer solution. Then the standard and sample absorbance was measured at 292 nm using UV–Visible spectrophotometer.

1.6.4 Transmission electron Microscopy (TEM) & Scanning electron microscopy (SEM):

The surface morphology of the prepared ATZ–GNPs (GLN–7) was studied using TEM (TECHNAI– Fei, Elec– tron optics, USA). ATZ–GNPs (GLN–7) dispersion was applied in the form of a droplet to the carbon–coated grids and dried at room temperature. The image of the NPs was taken at a 200 kV accelerated voltage ^{4,5}. Scanning electron microscopy (SEM) To create this scanning electron microscope image, gold nanoparticles were dispersed in a drop of sample which then dried on a glass microscope slide. Size: These gold nanoparticle are each about 200 nm in diameter. Imaging tool: Scanning electron microscope. (JCM–7000 Benchtop SEM – EDS)

1.6.5 XRD Analysis:

XRD analysis was done to evaluate the crystalline structure of ATZ and ATZ–GNPs (GLN–7) using a diffractometer (Rigaku X–ray diffractometer, Japan). The sample was measured at an applied current of 30mA, accelerating voltage 40 kV in a 2 θ angle configuration with CuK α radiation ($k = 1.54 \text{ \AA}$). The sample was scanned with a scanningrate of 2 $^\circ$ /min, in the measurement range of 20 $^\circ$ to 80 $^\circ$.^{5,13}

1.6.6 Drug Release:

Dialysis membrane method was used to determine the release of ATZ from the NPs formulations. Freshly made ATZ NPs were separated from the aqueous NPs suspension medium through ultra centrifugation. These NPs were dried at room temperature for 12 h. NPs equivalent to one dose of ATZ (400 mg) were then place in a capsule. In–vitro dissolution studies of pure drug and GLN–7 loaded in capsule were evaluated using a USP type–II apparatus. The dissolution basket was filled with 900ml of 7.4 pH phosphate buffer at 37 \pm 0.5 $^\circ$ C with a paddle rotation speed of 50 rpm using an 8 station dissolution apparatus, the 5ml of sample was taken at 1,2,3,4,6,10,12,16,24 hours and replaced with 5ml of fresh dissolution medium to keep the volume constant and maintained sink conditions. The drug release from the GLN–7 formulation was compared with the pure drug. The drug concentration in the released sample was determined by using UV–spectrophotometer at 292 nm. All the procedures were carried out three times. The released data were fitted into different mathematical models to determine the release mechanism^{7–9}

Drug release Kinetics:

An essential but challenging step is the investigation of the drug release mechanism from a pharmaceutical dosage form. Either zero order kinetics or first order kinetics were used to explain the order of drug release. The Higuchi, erosion, and Peppas equations were used to analyse the drug release mechanism.

Zero order release kinetics:

It defines a linear relationship between the fraction of drug released versus time. Zero order kinetics are described in Eq. 4.1.

$$C = K_0 t \quad (4.1)$$

where, K_0 is the zero-order release rate constant and C is the percentage drug released at time t . If the drug release follows zero order kinetics, a plot of the percentage drug release vs time will be linear.

First order release kinetics: Wagner hypothesised that drug release from the majority of slow-release tablets could be satisfactorily represented by apparent first order kinetics by assuming that the exposed surface area of a tablet reduced exponentially with time during the breakdown process. The first order kinetics can be described by using Eq. 4.2.

$$\log C = \log C_0 - K_1 t / 2.303 \quad (4.2)$$

where, C is the percentage of drug released at time (t) and K_1 is the first order release rate constant. A plot of the logarithm of percentage of drug remained against time will be linear if the release follows first order release kinetics. 3.4.3.

Higuchi equation: The active fraction released per unit of surface (Q) is defined as having a linear dependence on the square root of time. The Higuchi model's explanation is given by the Eq. 4.3.

$$Q = KHt^{1/2} \quad (4.3)$$

Where KH is the Higuchi diffusion coefficient and Q is the percentage of the drug released at time t . A plot of the percentage of drug released against square root of time will be linear, if the drug release complies with the Higuchi equation. Hixson and Crowell equation (4.4): This formula establishes the drug release based only on tablet degradation. The erosion equation is

$$Q = 1 - (1 - KEt)^3 \quad (4.4)$$

Where, Q is the percentage of drug released at time t , KE is the Hixson and Crowell constant. A plot between $[1 - (1 - Q)^{1/3}]$ against time will be linear if the release obeys erosion equation.

Korsmeyer-Peppas equation: Korsmeyer-Peppas support the drug release mechanisms for further judgement. $M_t / M_\infty = Kt^n$ (4.5) Where, M_t / M_∞ is the fraction of drug released at time t , K is the Korsmeyer-Peppas constant and 'n' is the release exponent. According to Korsmeyer-Peppas equation, the release exponent 'n' value is used to characterize different release mechanisms for a dosage form with cylindrical shape which are summarized as below. If the exponent $n = 0.45$, the drug release mechanism is Fickian diffusion, and if $0.45 < n < 0.89$, the drug release mechanism is non-Fickian or anomalous diffusion. Case-II Transport or typical zero-order release is indicated by an exponent value of 0.89.

1.6.7 Antibacterial activity:

The minimum inhibitory concentration of ATZ-GNPs (GLN7) was evaluated in LB (Lysogeny broth) medium against the gram-positive organism (*S. aureus*) and gram-negative LB organism (*E. coli*). ATZ-GNPs of different concentrations (0, 1, 5, 10, 20 $\mu\text{g/mL}$) were added to the medium with bacterial cultures load of 10^5 –

10^6 CFU/mL and then incubated at 35°C . The optical density of each sample was measured after 24 h to evaluate the minimum inhibitory concentration (MIC) ⁹. Further, the sample was evaluated for antibacterial activities of *S. aureus* and *E. coli* bacteria using the agar well diffusion process.¹⁰ Before being tested, the bacteria were kept in broth and sub-cultured in a Petridish. The test

sample ATZ- GNPs were added to sterile Mueller Hinton plates well. The positive control gentamycin (0.1 mg/mL) was taken to compare the result. The plates were incubated for 24 and 48 h in an incubator and inhibition zones diameter (mm) was determined in triplicate.

2. RESULTS AND DISCUSSION

2.1 Standard calibration curve of Atazanavir:

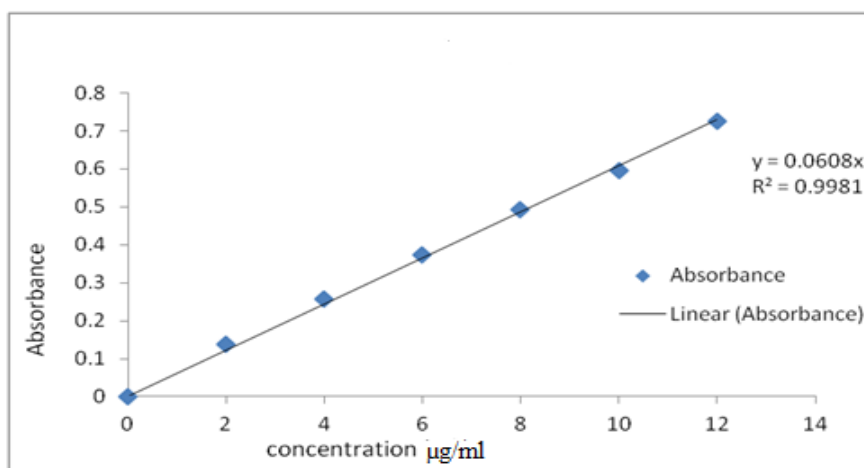


Figure 2.1: Standard calibration curve of Atazanavir in pH 7.4

DISCUSSION:

The linearity was found to be in the range of 2–12 µg/ml in acetone, pH 7.4 buffer. The regression value was closer to 1 indicating the method obeyed Beer–lamberts’ law.

2.2 Drug excipient compatibility:

Drug and excipient compatibility was confirmed by comparing spectra of FT–IR analysis of pure drug with that of various excipients used in the formulation.

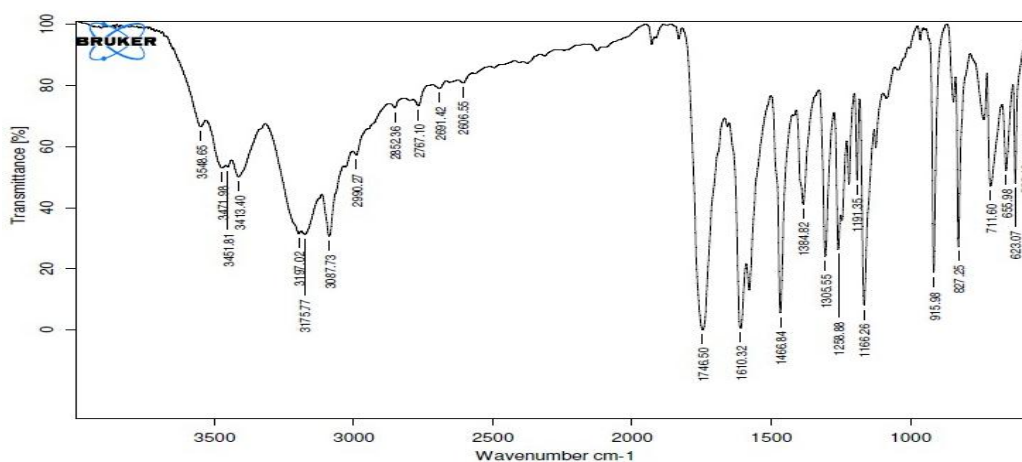


Figure 2.2: FTIR spectrum of Atazanavir Optimized Formulation

Discussion: From the drug excipient compatibility studies we observe that there are no interactions between the pure drug (Atazanavir) and optimized formulation (Atazanavir + excipients) which indicates there are no physical changes.

2.3 Optimization:

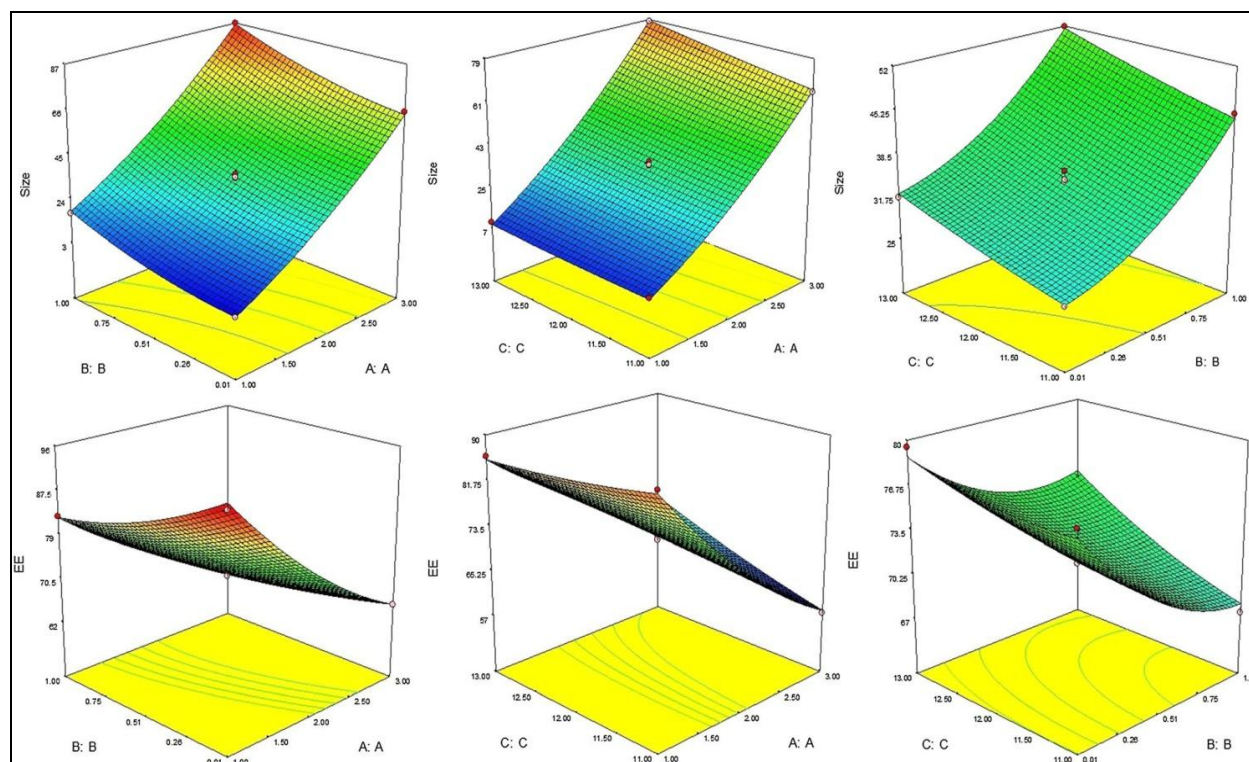


Fig.2.4: 3D contour plot showing the effect of independent variables on dependent variables particle size (Y^1) and encapsulation efficiency (Y^2).

The polynomial equation shows that the independent variables have individual as well as combined effects on the PS. ANOVA of individual terms of the PS equation revealed that the factors A,B,C,AB,AC,BC,A²,B²,and C² are found to be significant model terms. Additionally, both hydrophilic polymers (gold chloride and pectin; factors A and C) showed a positive impact on the PS. A rise in gold chloride concentration (A) resulted in a larger globule size in the primary suspension. An increase in pectin concentration (B), also depicted an increase in PS. At higher concentration, the pectin adsorption increases on the particle surface of the primary suspension, and thus a larger size of gold NPs. Furthermore, during the formation of the primary suspension, the pH range (C) had a major negative impact on the size, i.e., an increase in pH range resulted in a decrease in PS of the primary suspension, which in turn directed the formation of smaller size NPs. The findings were also significantly influenced by the other combined interaction terms (AB, BC, and AC). A change in one-factor magnitude will almost certainly affect the response generated by changes in other factors. All statistically relevant higher-order terms (A², B², and C²) has a non-linear relationship with the PS of the NPs.²

2.4 Effect on Encapsulation Efficiency (Y^2):

The independent factors gold chloride (A), pectin (B) and pH (C) showed a significant effect on the EE. The mini-mum EE of 57.4% is shown by the formulation (GLN-2) having the composition: gold chloride (2 mM), pectin (0.5%) and pH-12. The maximum encapsulation efficiency of 94.1% was observed for the formulation (GLN-7) having the composition: gold chloride (1 mM), pectin (0.01%) and pH-12. The variation in the EE was observed due to the variation in the composition of independent variables. The effect of independent variables on the EE could be well observed by the polynomial equation and 3D response surface plot (Fig. 1). The quadratic equation governing the encapsulation efficiency of the gold NPs is as follows:

$$\% EE = +71.83 - 1.92A - 3.39B + 1.97C + 2.97AB$$

$$+3.74AC+1.15BC+3.07A^2+2.13B^2$$

$$+0.64C^2 \text{ A,B,C,AC,AC,A}^2\text{,B}^2\text{,C}^2$$

These are all significant model terms ($p < 0.05$) as shown by the polynomial equation and ANOVA results.³ The concentration of gold chloride (A) and pectin concentration (B) have shown a negative influence on EE. With the increase in gold chloride concentration (A) and pectin concentration (B), the EE was decreased. It may be due to the highly lipophilic character of the drug (ATZ). The variable (A) has shown a greater effect than variable B. But the third variable 'pH' (C) showed a positive effect on EE. A higher pH might have led to enhanced encapsulation from the hydrophilic gold coating. The other combined interaction terms (AB, BC, and AC) were also found to have a significant positive effect on the results. The combined factors (gold chloride and pectin, AB) have shown a positive effect on encapsulation efficiency. The combination of these factors helps to get greater encapsulation of ATZ in the specific ratio. A similar effect is obtained by the blend of gold chloride (A) and pH of the solution (C) as well as pectin (B) and pH (C). The factors AC and BC have shown greater effect than the factor AB. A change in one-factor magnitude will almost certainly influence the response produced by other factors. All statistically significant higher-order terms (A^2 , B^2 , and C^2) was found to have an on linear relationship with encapsulation efficiency. The polynomial equation interpretation is well supported with the 3D-response surface graph (between encapsulation efficiency and various factors)⁴.

2.5. Point Prediction:

To get the minimum PS and maximum EE, the software used the point prediction method to select optimized composition. Out of 15 formulations given by the software, the formulation (GLN-7) having the composition: gold chloride 1 mM (A), pectin 0.1% (B) and pH 12 (C) showed the PS of 3.1 nm with an EE of 94.1%. The optimized formulation (GLN-7) prepared with the composition: gold chloride 1 mM (A), pectin 0.1% (B) and pH 12 (C), showed the PS of 3.9 ± 0.1 nm with an EE of $97.2 \pm 3.9\%$. The software generated predicted PS and EE were found to be 3.8 nm and 95.6% respectively. The close results of actual and predicted values confirm that the user process is accurate. The predicted and actual attribute of the optimized formulation is shown in Table 2. The overall desirability for each factor was found to be closer to unity (0.95 and 0.98) for size and encapsulation efficiency. The statistical analysis was also found well in agreement with the point prediction value of each factor. The statistical analysis of the size and encapsulation efficiency is pre-sented in Table3. Among the four statistical parameters, the best-fit model was found to be for the quadratic model⁵.

Table 2.2: Predicted and actual values of the optimized ATZ gold nanoparticles (GLN-7)

Formulation	Composition			Characterization	
	Gold chloride (X ¹)	Pectin (X ²)	pH (X ³)	Particle size(nm)	Encapsulation Efficiency (%)
GLN-7(predicted)	1.1 mM	0.2%	12.5	3.8	95.6%
GLN-7(actual)	1 mM	0.1%	12	3.9 ± 0.2	97.2 ± 3.9
% Error	-	-	-	0.27	1.67

2.6. Characterization:

2.6.1 Particle Size (PS):

The mean particle size range of the ATZ gold NPs was found in the range of 3.1 nm (GLN-7) to 65.3 nm (GLN- 2). The optimized ATZ gold NPs showed the PS of 3.9 ± 0.1 nm.

2.6.2 Polydispersity Index (PDI):

The optimized ATZ gold NPs showed a low polydispersity index (PDI) value of 0.5 ± 0.1 , indicating the uniform particle size distribution which is ideal for the greater drug release due to the smaller particle size distribution.

2.6.3 Surface Charge (ZP):

Surface charge of -33.1 ± 0.5 mV (Fig.5.5 , 5.6).The significant variations in the PS are due to the change in the composition of independent variables.

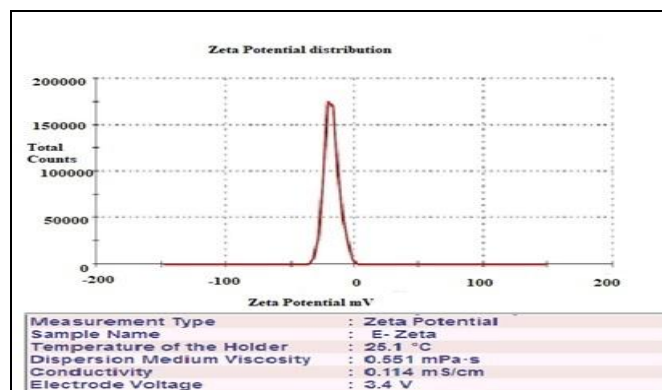


Figure 2.5: zetapotential

2.7 .Encapsulation efficiency:

GLN-7 showed encapsulation efficiency of $97.2 \pm 3.9\%$, indicating that the experimental process and structure are suitable for the encapsulation of a high concentration lipophilic drug in the hydrophilic gold chloride (AuCl_4) (Table 2). One of the primary targets for improving encapsulation efficiency is the outer layer of hydrophilic pectin that protects the ATZ from oozing out.⁶

2.8 Percentage Yield:

The optimized formulation GLN-7 percentage yield was found to be $92.5 \pm 2.4\%$, indicating the low process loss. The increase in pectin concentration will influence it, and hence a improved practical yield.

2.9. Drug Content: The percentage of drug content was calculated. The GLN - 7 showed drug content 99.86 ± 0.12 .

2.10. Transmission electron Microscopy (TEM):

TEM analysis revealed that the ATZ gold NPs (GLN-7) are spherical in shape with no aggregation (Fig.5.7). This is due to the capping of pectin which stabilized the individual NPs.

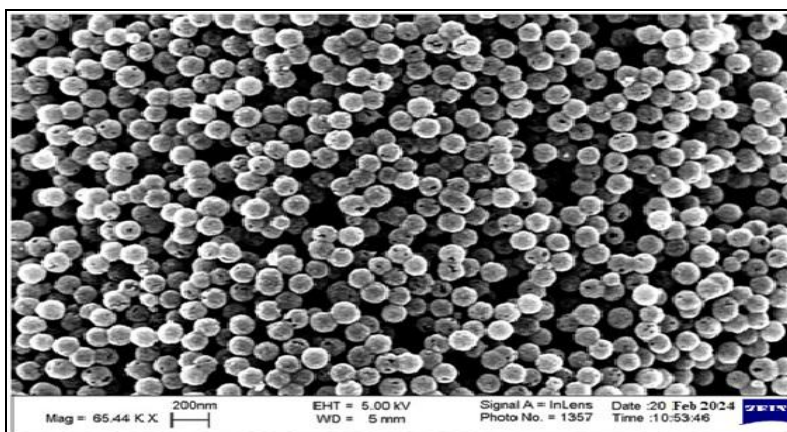


Figure: 2.6 SEM Image of Atazanvir nanoparticles

2.11 SEM Analysis: The results of SEM analysis confirm the prepared nanoparticles were spherical in shape and nano in size and smooth surface SEM image shown in fig: 5.8

5.12 X-Ray Diffraction:

The powder XRD diffractogram of ATZ (drug), gold nanoparticles (GNPs) and ATZ gold NPs (GLN-7) are depicted in Fig. 5.9. The presence of intense diffraction peaks indicates the formation of crystalline gold (Au). The presence of AuNPs peaks were reflected radiation (Bragg peaks) at 31.3°, 45.3°, 65.9° and 74.9° corresponding to characteristic diffractions of (111), (200), (220) and (311) planes. ATZ showed the peaks at 6.8°, 15.9°, 18.5°, 20.8°, 23.9°, 26.4°, and 28.9° and ATZ gold NPs (GLN-7) showed the peaks at 6.8°, 28.4°, 34.3°, 43.6°, 65.3°, and 74.9°, respectively. The mean average size of crystals was calculated using the Debye-Scherrer Equation. The line width of (111) plane was considered for the calculation. The Debye-Scherrer equation is given as follows:⁷

$$d = \frac{k\lambda}{\beta \cos \theta}$$

where, 'd' is the mean size of the crystalline domains, 'k' is dimensionless shape factor, with a value close to unity (0.9), 'k' is a wavelength of X-ray, 'β' is the width at half-maximum of the (111) peak in radians, 'θ' is the angle of diffraction. The size of crystal of ATZ gold NPs (GLN-7) determined by the given equation was found to be in the range of 3–14.0 nm. The estimation of size using the equation was in confirmation with diameter of synthesized gold NPs (AuNPs) obtained from TEM.



Figure 2.7: XRD patterns of A. Azatanvir, B. blank gold nanoparticles and, C. ATZ load gold nanoparticles (GLN-7)

2.13 DSC Studies:

DSC Thermogram of Atazanvir and Atazanvir nanoparticles Drug-Excipients accelerated compatibility study-Physical observation and assay were shown in fig.5.10. DSC of Atazanvir showed a sharp endothermic peak at about 211 °C (melting point). The physical mixture of Atazanvir with other excipients also showed the same thermal behavior (207 °C) as the individual component. DSC results also revealed that the physical mixture of Atazanvir with excipients showed superimposition of the thermogram. There was no significant change observed in melting endotherm of physical mixture of Atazanvir and excipients. Hence from the DSC study, it was found that there was no interaction between Atazanvir and other excipients used in the

formulation.

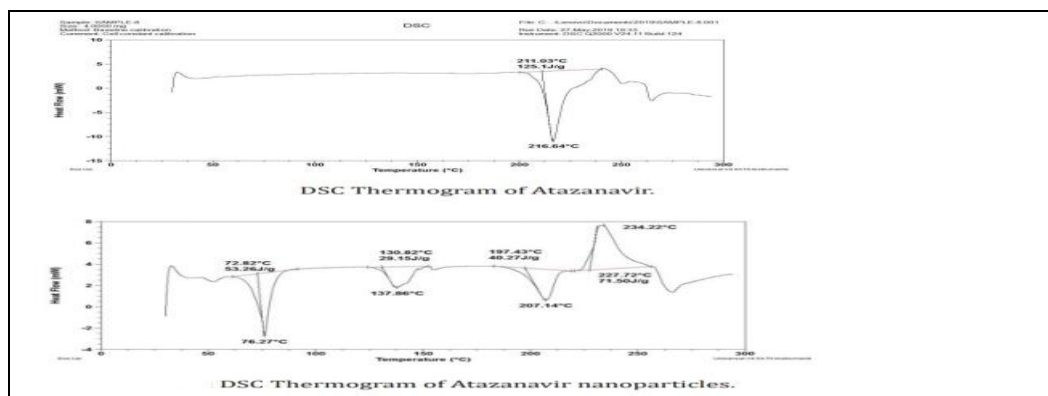


Figure: 2.8 DSC Thermogram of Atazanavir and Atazanavir nanoparticles

2.14 In vitro drug release studies:

The in vitro drug release studies are conducted at pH 7.4 of pure drug (ATZ suspension) form and compare with gold nanoparticle (GLN-7) formulation the results are shown in following figure

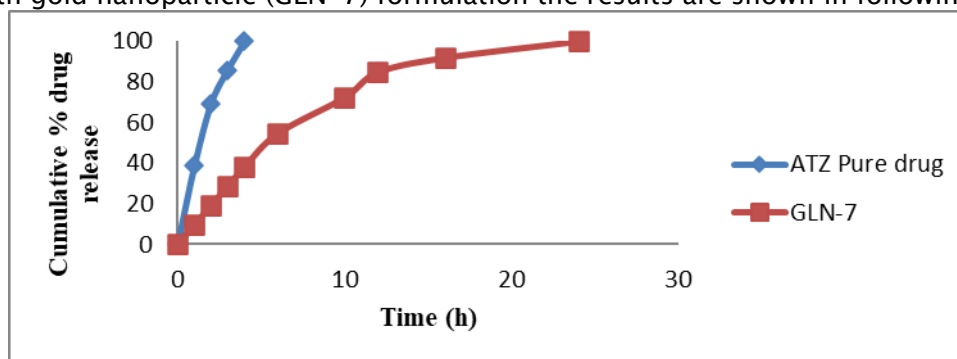


Fig: 2.11 In-vitro release of ATZ pure drug and ATZ gold nanoparticle (GLN-7) at two different pH 7.4

2.15 In vitro drug release result and discussion:

Figure shows the comparison of ATZ release from ATZ pure drug and ATZ gold nanoparticles (GLN-7) in phosphate buffer (pH7.4). ATZ release from the pure drug was observed to be $99.81 \pm 0.08\%$ within 4 h of study. However, ATZ release from gold NPs (GLN-7) showed $99.84 \pm 0.23\%$ release in 24 h. The relative release profile of media demonstrated that the drug dissolution behaviour is affected by pH.⁸

2.16 In vitro drug release kinetic studies:

Table 2.3: In vitro drug release model fitting for ATZ gold NPs (GLN-7) in different release media

Formulation	Zero order		First order		Higuchi		Korsmeyer peppas	
	R ²	K ₀	R ²	K ₁	R ²	k	R ²	n
GLN-7	0.953	24.67	0.399	-0.075	0.985	50.76	0.959	0.9856
ATZ pure drug	0.873	4.356	0.095	-0.207	0.965	24.15	0.500	0.2378

The drug release mechanism was calculated, and the best model was chosen based on the highest values of regression coefficients (actual and adjusted), as seen in fig 2.12–2.15, Table 2.5 The best-fitting model in both the media was found to be the Korsmeyer–Peppas model in pH 7.4 media. Korsmeyer–Peppas model is used to describe and analyze the release of a drug from a

polymeric nanoparticles dosage form such, or when the release follows several kinetics mechanisms also, used when the controllable process mechanism is incomprehensible, such as a combination more than one type of release mechanism or is a combination of the diffusion of the active principle (Fickian transport) and Case II transport ATZ has a continuous release of GLN-7 would be beneficial. As a result, this mechanism is capable to control the drug release.⁹

2.17 Antibacterial Activity: The Minimum inhibitory concentration (MIC) level of the ATZ gold nanoparticles (GLN-7) was evaluated against E.coli (Gram-negative bacteria) and S. aureus (Gram-positive bacteria). The different concentration was evaluated to select the one concentration and further assessed for antibacterial activity. The inhibition kinetics of the different concentrations of ATZ gold NPs were evaluated in E.coli and S. aureus as shown in Fig15. MIC of the ATZ-gold NPs was found to be 10lg/mL for both S.aureus and E.coli. At high concentration, the viable cells were inhibited within 2.5 and 3 h for E. coli and against S. aureus, it showed the inhibition within 2 and 3 h. 5 ppm concentration was not enough to inhibit both organisms within tested time. The gold nanoparticles showed a lower MIC value over GLN-7, due to the smaller size of the nanoparticles and the negative surface charge of pectin interferes with microbial absorption on the surface of gold nanoparticles. It was reported in S.M. Navarro Gallon., et al. that the narrow size of nanoparticles influenced the antibacterial activity due to the specific surface area for interaction with the bacterial membrane.¹⁰ Log Colony forming units (CFU) per milliliter vs time The antibacterial activity of ATZ gold nanoparticles(GLN-7) was evaluated against E. coli and S. aureus, in a fixed-dose for different time points and result shown in Fig.2.15,2.16 and table 2.5,2.6.

Table: 2.4 The antibacterial activity of ATZ gold nanoparticles (GLN-7) was evaluated against E. coli in a fixed-dose for different time points

S.No	Time (h)	control	1 µg/ml	5 µg/ml	10 µg/ml	20 µg/ml
1.	0	6	6	6	6	6
2.	0.5	6	5.5	5.3	5	4.5
3.	1	6	5	4	4	3
4.	1.5	6	4.9	3.5	3	1.5
5.	2	6	4.8	3	2	0.5
6.	2.5	6	4.7	2	1	0
7.	3	6	4.6	1.5	0	0
8.	4	6	4.5	1	0	0
9.	5	6	4.4	0.5	0	0
10.	6	6	4.3	0	0	0

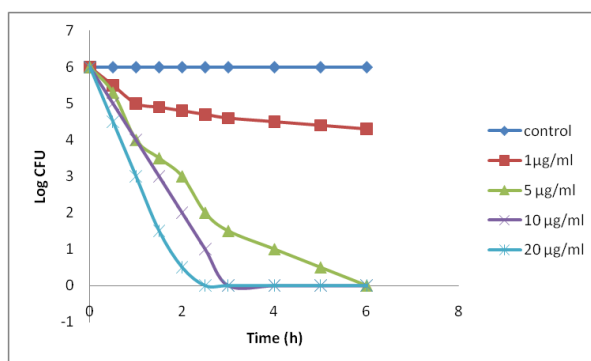


Fig: 2.19. The antibacterial activity of ATZ gold nanoparticles (GLN-7) was evaluated against E. coli in a fixed-dose for different time points

Table: 2.7 The antibacterial activity of ATZ gold nanoparticles (GLN-7) was evaluated against *S. aureus*, in a fixed-dose for different time points

S.No	Time (h)	control	1 µg/ml	5 µg/ml	10 µg/ml	20 µg/ml
1.	0	6	6	6	6	6
2.	0.5	6	5	5	5	4.5
3.	1	6	4.8	4.5	4	3
4.	1.5	6	4.7	3.5	3	2
5.	2	6	4.6	3	2	0.8
6.	2.5	6	4.5	2.5	1	0.3
7.	3	6	4.5	2	0.4	0
8.	4	6	4.4	1.5	0.2	0
9.	5	6	4.3	0.5	0	0
10.	6	6	4.4	0	0	0

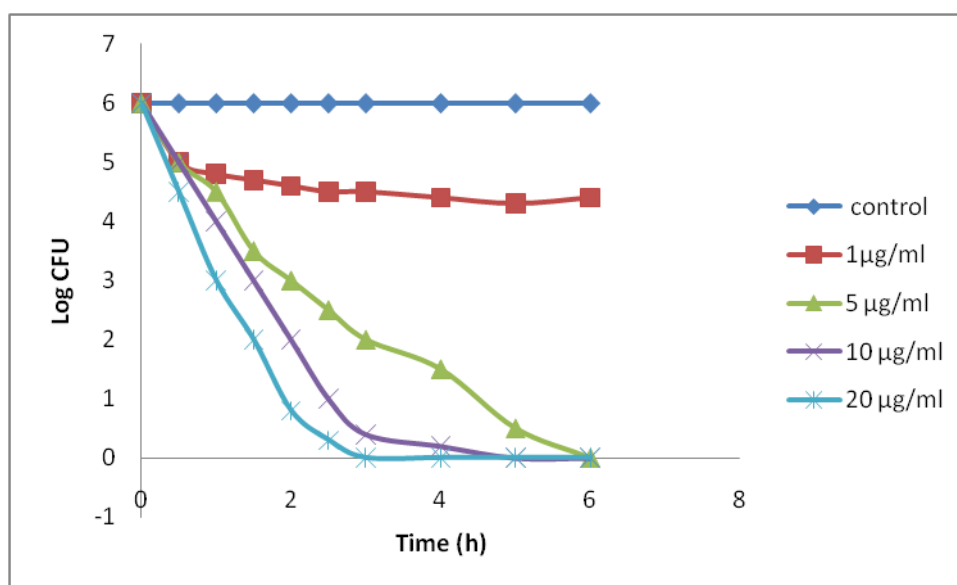


Fig: 2.20 The antibacterial activity of ATZ gold nanoparticles (GLN-7) was evaluated against *S. aureus*, in a fixed-dose for different time points

2.17.1 Zone of inhibition study:

The growth of the bacteria is treated, as well as untreated well with gold nanoparticles was investigated. The standard gentamycin showed the ZOI of 14.3 ± 1.8 mm at 24h and 11.7 ± 0.8 mm at 48 h. The antibacterial effect was found to be higher at 24 h than 48 h. In the case of pure ATZ, a similar type of effect was found with standard gentamycin. The sample showed a higher effect at 24 h (12.6 ± 1.3 mm) than 48 h (10.9 ± 0.7 mm). ATZ gold NPs showed a higher effect at 48 h (14.0 ± 0.8 mm) than 24 h (16.3 ± 1.3 mm). The greater effect may be due to the slower release of ATZ from gold NPs as well as gold also reported for the antibacterial property. The presence of gold chloride and ATZ showed synergistic effect on the tested organisms. The gold NPs adsorb on the surface of bacteria and inhibit the intracellular enzymatic activity. The zone of inhibition was also evaluated against *E. Coli* and the result showed a similar type of effect (Fig.17). The zone of inhibition against *E. coli* after treatment with standard Gentamycin, pure ATZ and ATZ-NPs (GLN-7) were found to be 17.1 ± 2.6 mm, 12.5 ± 1.3 mm, and 14.4 ± 2.3 mm, respectively at 24 h. The same concentration was also evaluated for 48 h and the result depicted significant ($p < 0.05$) changes in the results. The standard gentamycin showed a smaller zone of inhibition with 14.1 ± 1.3 mm, pure ATZ also revealed lesser effect (9.6 ± 0.8 mm) than 24 h treated well. In the case of ATZ gold nanoparticles (GLN-7), the enhanced effect was observed at both time points

than pure ATZ. At 24 h, the ZOI was found to be 14.4 ± 2.3 mm and at 48 h, the ZOI was found to be 15.9 ± 1.6 mm. ATZ gold nanoparticles (GLN-7) showed prolonged effect due to the slower ATZ release from the gold NPs. The other reason for the enhanced effect is the antibacterial activity of the gold which gives synergistic action to the drug ATZ. CD4 which are susceptible to HIV infection. It was observed that as the concentration of gold nanoparticles increases the cytotoxicity increases as well. When compared to the control group with ATZ gold nanoparticles demonstrated higher cell viability. As a result, the encapsulation of the drug has little impact on the in-vitro cytotoxicity of gold nanoparticles. The ATZ gold nanoparticles (GLN-7) were found to be non-toxic and suitable for in-vivo applications.

In vivo pharmacokinetic evaluation:

The aim of this pharmacokinetic investigation is to achieve and sustain an effective drug concentration at the target receptor site. As the body continuously attempts to eliminate the drug it becomes essential to strike a balance between drug absorption and elimination to maintain the desired drug concentration in the blood plasma. The circulation of blood throughout the body enables drug distribution, which usually occurs at a faster rate than drug absorption or elimination. The systemic absorption of pharmaceutical dosage forms involves a series of metabolic processes, including drug dissolution in the gastrointestinal tract and drug absorption across the cell membrane into the systemic circulation. The drug, once absorbed is then transported through the bloodstream to its site of action, where it binds to receptors, resulting in a pharmacological effect.

Conducting pharmacokinetic studies is of utmost importance during product development. Therefore, the primary objective of this study is to perform pharmacokinetic assessments for the newly formulated dosage form. After selecting the most suitable in vitro optimised formulation, it was chosen for pharmacokinetic evaluation using rabbits as the animal model. This approach allows us to predict the drug bioavailability and various pharmacokinetic parameters. the formulations.

7.6.1 In vivo pharmacokinetic parameters:

Table 7.5: Pharmacokinetic parameters

Parameters	ATZ oral Solution	ATZ optimized formulation
C _{max} (ng/ml)	0.32 ± 0.17	0.87 ± 0.24
T _{max} (hr)	3.14 ± 1.82	13.80 ± 0.15
AUC ₀₋₂₄ (ng.hr/mL)	2.46 ± 1.2	11.83 ± 0.23
T _{1/2} (hr)	6.39 ± 1.5	14.78 ± 1.7

Optimized formulation (GLN-7) indicated that the pharmacokinetic profile was more reproducible than that of pure drug. Plasma drug profile of OPT formulation exhibited more sustained release vis-a-vis pure drug. On the whole, the values of C_{max} and AUC₀₋₂₄ rose considerably vis-a-vis pure drug to 2.71 and 4.80-fold, respectively, in case of the OPT formulation ratifying distinct improvement in extent of bioavailability.

Conclusion:

The present research work was designed to prepare ATZ loaded gold nanoparticles. The formulations were optimized using Box Behnken design. The prepared ATZ gold nanoparticles (GLN-7) showed a narrow particle size, higher encapsulation efficiency and The drug release from

ATZ pure drug and ATZ gold nanoparticles (GLN-7) in phosphate buffer (pH7.4). ATZ release from the pure drug was observed to be $99.81 \pm 0.08\%$ within 4 h of study. However, ATZ release from gold NPs (GLN-7) showed $99.84 \pm 0.23\%$ release in 24 h. SEM and TEM study result depicted smooth surface morphology. GLN-7 showed better antimicrobial activity against Gram-positive (*E. coli*) and Gram-negative (*S.aureus*) bacteria. The pharmacokinetic investigation aimed to achieve and sustain effective drug concentrations at the blood plasma and the developed in-situ floating gel formulation of Atazanvir demonstrated promising characteristics. The study successfully struck a balance between drug absorption and elimination to maintain desired drug concentrations in the blood plasma. The optimized formulation exhibited controlled drug release, leading to a gradual decline in drug concentration over time and prolonged drug release in the blood stream compared to the reference product. The in vivo pharmacokinetic evaluation revealed significant differences in the pure drug and optimized formulation. The mean peak plasma concentration (C_{max}) of optimized formulation GLN-7 showed 2.71 folds increase than the pure drug. It indicates that the optimised formulation effectively controlled the amount of drug release. The mean T_{max} of test formulation showed longer (13.80 hours) than the T_{max} of pure drug (3.14 hours). It shows that the optimized formulation showed an effective delayed peak plasma concentration. The Relative bioavailability of optimised formulation showed 4.80 folds increase than the pure drug. The optimised formulation showed longer $t_{1/2}$ than the reference product, test formulation showed slower elimination rate than that of reference product, indicating its favorable drug release profile and enhanced pharmacological effect. Overall, the optimized in-situ floating gel formulation of Atazanvir exhibited promising pharmacokinetic behavior, with sustained drug release and enhanced bioavailability. Based on the above mentioned parameters GLN -7 effectively release the drug release in a controlled manner through the prepared gold nanoparticles, These findings hold significant potential for the future development and clinical applications of this dosage form as a gastro retentive system for achieving prolonged drug release and improved therapeutic efficacy.

References:

1. Cai W, Gao T, Hao Hong JS. Applications of gold nanoparticles in nanotechnology. *Nanotechnol Sci Appl*. 2008;1:17–32. doi:10.2147/NSA.S3788.
2. Mokhatab S, Fresky MA, Islam MR. Applications of nanotechnology in oil and gas E&P. *J Pet Technol*. 2006;58(04):48–51. doi:10.2118/0406-0048-jpt.
3. Mu L, Sprando RL. Application of nanotechnology in cosmetics. *Pharm Res*. 2010;27(8):1746–1749. doi:10.1007/s11095-010-0139-1.
4. Inès Hammami Review Gold nanoparticles: Synthesis properties and applications, *Journal of King Saud University – Science*, *Journal of King Saud University – Science* 33 (2021) 101560.
5. Ealias AM, Saravanakumar MP. A review on the classification, characterisation, synthesis of nanoparticles and their application. *IOP Conf Ser Mater Sci Eng*. 2017;263:3. doi:10.1088/1757-899X/263/3/032019.
6. Daniel M-C, Astruc D. Gold nanoparticles: assembly, supramolecular chemistry, quantum-size-related properties, and applications toward biology, catalysis, and nanotechnology. *Chem Rev*. 2004;104 (1):293–346.
7. Park JW, Benz CC, Martin FJ. Future directions of liposome- and immunoliposome-based cancer therapeutics. *Semin Oncol*. 2004;31 (SUPPL. 13):196–205. doi:10.1053/j.seminoncol.2004.08.009.

8. Jurgons R, Seliger C, Hilpert A, Trahms L, Odenbach S, Alexiou C. Drug loaded magnetic nanoparticles for cancer therapy. *J Phys Condens Matter*. 2006;18(38):38. doi:10.1088/0953-8984/18/38/S24.
9. Dykman L, Khlebtsov N. Gold nanoparticles in biomedical applications: recent advances and perspectives. *Chem Soc Rev*. 2012;41(6):2256–2282. doi:10.1039/c1cs15166e..
10. Paciotti GF, Kingston DGI, Tamarkin L. Colloidal gold nanoparticles: a novel nanoparticle platform for developing multifunctional tumor-targeted drug delivery vectors. *Drug Dev Res*. 2006;67(1):47–54. doi:10.1002/ddr.20066.
11. Chaurasia G. A review on pharmaceutical preformulation studies in formulation and development of new drug molecules. *International journal of pharmaceutical sciences and research*. 2016;7(6):2313–2320.
12. Chaurasia G. A review on pharmaceutical preformulation studies in formulation and development of new drug molecules. *International journal of pharmaceutical sciences and research*. 2016;7(6):2313–2320.
13. Myrdal PB, Yalkowsky SH. Solubilization of drugs in aqueous media. In: Swarbrick J, editor. *Encyclopedia of Pharmaceutical Technology*. 3rd edition. New York, NY, USA, : Informa Health Care; 2007. p. p. 3311
14. Chadha R, Bhandari S. Drug - excipient compatibility screening - role of thermoanalytical and spectroscopic techniques. *Journal of pharmaceutical analysis*. 2014; 87:82–97.
15. Jorgensen WL, Duffy EM. Prediction of drug solubility from structure. *Adv Drug Deliv Rev*. 2002;54:355–366.
16. Llinas A, Glen RC, Goodman JM. Solubility challenge: can you predict solubilities of 32 molecules using a database of 100 reliable measurements? *J Chem Inf Model*. 2008;48(7):1289–1303.
17. S. R. K. Yellela, "Pharmaceutical technologies for enhancing oral bioavailability of poorly soluble drugs," *Journal of Bioequivalence & Bioavailability*, vol. 2, no. 2, pp. 28–36, 2010.
18. J. Turkevich, P. C. Stevenson, and J. Hillier (1951). *Discuss. Faraday Soc.* 11, 55.
19. Sultan akthar, Formulation of gold nanoparticles with hibiscus and curcumin extracts induced anticancer activity. *Arabian journal of chemistry*, Volume 15, Issue 2, February 2022, 103594.
20. Leila fotooh abadi, Tenofovir - tethered gold nanoparticles as a novel multifunctional long - acting anti- HIV therapy to over come deficient drug delivery: an in vivo proof of concept. *J Nanobiotechnol* 21, 19 (2023).
21. Poornima rawat, Formulation of Cabotegravir loaded gold nanoparticles; Optimisation, characterization to In vitro cytotoxicity study. *National library of medicine*, 2023; 34(2): 893–905.
22. I.Capek (2017). *Adv. Colloid Interface Sci.* 249, 386.
23. S.D.Mahajan, R.Aalinkeel, W.C.Law, J.L.Reynolds, B.B.Nair, D.E.Sykes, K.T.Yong, I.Roy, P.N.Prasad, and S.A.Schwartz (2012). *Int. J. Nanomed.* 7, 5301.
24. A.Z.Nurakhmetova, A.N.Azhkeyeva, A.I.Klassen, and S.G.Tatykhanova (2020). *Polymers* 12, 2625.
25. E.Boisselier, A.K.Diallo, L.Salmon, C.Ornelas, J.Ruiz, and D. Astruc (2010). *J. Am. Chem. Soc.* 132, 2729.

26. Clinical info HIV gov by AIDS Research Advisory Council (OARAC). Guidelines for the Use of Antiretroviral Agents in Adults and Adolescents with HIV.
27. Jorgensen WL, Duffy EM. Prediction of drug solubility from structure. *Adv Drug Deliv Rev.* 2002;54:355–366.
28. Llinas A, Glen RC, Goodman JM. Solubility challenge: can you predict solubilities of 32 molecules using a database of 100 reliable measurements? *J Chem Inf Model.* 2008;48(7):1289–1303.
29. S. R. K. Yellela, “Pharmaceutical technologies for enhancing oral bioavailability of poorly soluble drugs,” *Journal of Bioequivalence & Bioavailability*, vol. 2, no. 2, pp. 28–36, 2010.
30. M. Aulton, “Dissolution and solubility,” in *Pharmaceutics: The Science of Dosage form Design*, M. E. Aulton, Ed., p. 15, Churchill Livingstone, 2nd edition, 2002.
31. The United States Pharmacopeia, USP 30–NF 25, 2007.
32. British Pharmacopoeia, 2009.
33. G. L. Amidon, H. Lennernäs, V. P. Shah, and J. R. Crison, “A theoretical basis for a biopharmaceutic drug classification: the correlation of in vitro drug product dissolution and in vivo bioavailability,” *Pharmaceutical Research*, vol. 12, no. 3, pp. 413–420, 1995.
34. Higuchi T. Mechanism of sustained–action medication. Theoretical analysis of rate of release of solid drugs dispersed in solid matrices. *Journal of Pharmaceutical Sciences*, 1963;52:1145–1149. 102 16.
35. Hixson AW and Crowell JH. Dependence of reaction velocity upon surface and agitation. I. Theoretical considerations. *Industrial & Engineering Chemistry*, 1931 Aug;23(8):923–931.
36. Korsmeyer R, Gurny R and Peppas N. Mechanisms of solute release from porous hydrophilic polymers. *International Journal of Pharmaceutics*, 1983 May 1;15(1):25–35.
37. NA Peppas. Analysis of Fickian and non–Fickian drug release from polymers. *Pharmaceutica Acta Helvetiae*, 1985;60:110–111.
38. Harish joshi, Formulation and Evaluation of Nanoparticles Containing Antiviral Protease Inhibitor, *Mathews Journal of Pharmaceutical Science*, Received Date: January 02, 2023 Published Date: February 03, 2023.
39. . Balkundi S, Nowacek AS, Veerubhotla RS, Chen H, Martinez–Skinner A, Roy U, et al. (2011). Comparative manufacture and cell based delivery of antiretroviral nano formulations. *Int J Nanomedicine.* 6:3393–3404.
40. Beloqui A, Solinís MÁ, Gascón AR, del Pozo–Rodríguez A, des Rieux A, Prétat V. (2013). Mechanism of transport of saquinavir–loaded nanostructured lipid carriers across the intestinal barrier. *J Control Release* 166:115–123.
41. Bender AR, Von Briesen H, Kreuter J, Duncan IB, Rubsamen–Waigmann H. (1996). Efficiency of nanoparticles as a carrier system for antiviral agents in human immunodeficiency virus–infected human monocytes/ macrophages in vitro. *Antimicrob Agents Chemother* 4:1467–1471.
42. C. G. England and M. C. Miller, Ashani Kuttan, JO Trent, HB Frieboes (2015). *Eur. Jo. Pharm. Biopharm.* 92, 120.
43. S. Dash, P. N. Murthy, L. Nath, and P. Chowdhury (2010). *Acta Pol. Pharmaceut.* 67, 217.